Broken symmetry and pseudogaps in ropes of carbon nanotubes

Delaney, P., Choi, H. J., Ihm, J., Louie, S. G., & Cohen, M. L. (1999). Broken symmetry and pseudogaps in ropes of carbon nanotubes. Physical Review B (Condensed Matter), 60(11), 7899-7904. DOI: 10.1103/PhysRevB.60.7899

Published in:
Physical Review B (Condensed Matter)

Broken symmetry and pseudogaps in ropes of carbon nanotubes

Paul Delaney, Hyoung Joon Choi,* Jisoon Ihm,* Steven G. Louie, and Marvin L. Cohen
Department of Physics, University of California at Berkeley, Berkeley, California 94720
and Materials Sciences Division, Lawrence Berkeley National Laboratory, Berkeley, California 94720
(Received 12 February 1999)

We investigate the influence of tube-tube interactions in ropes of (10,10) carbon nanotubes, and find that these effects induce a pseudogap in the density of states (DOS) of the rope of width 0.1 eV at the Fermi level. In an isolated (n,n) carbon nanotube there are two bands that cross in a linear fashion at the Fermi level, making the nanotube metallic with a DOS that is constant in a 1.5 eV wide window around the Fermi energy. The presence of the neighbouring tubes causes these two bands to repel, opening up a band gap that can be as large as 0.3 eV. The small dispersion in the plane perpendicular to the rope smears out this gap for a rope with a large cross-sectional area, and we see a pseudogap at the Fermi energy in the DOS where the DOS falls to one third of its value for the isolated tube. This phenomenon should affect many properties of the behavior of ropes of (n,n) nanotubes, which should display a more semimetallic character than expected in transport and doping experiments, with the existence of both hole and electron carriers leading to qualitatively different thermopower and Hall-effect behaviors from those expected for a normal metal. Band repulsion like this can be expected to occur for any tube perturbed by a sufficiently strong interaction, for example, from contact with a surface or with other tubes. [S0163-1829(99)00335-5]

I. INTRODUCTION

Single-walled carbon nanotubes[1] are tubular structures that are typically nanometers in diameter and many microns in length. They can be formed by cutting a graphene sheet along two parallel lines and then rolling up the sheet so that the cut edges are brought next to each other. Two interesting properties of the tubes are their mechanical strength and geometry-driven electronic properties. As could be expected from the high in-plane stiffness of a graphene sheet, the tubes are very strong materials. As regards the electronic structure, depending on the angle of the cut and on the diameter of the resulting tube, one may obtain metallic, small-gap, or insulating materials.[2–4] In particular, the metallic or *armchair* tubes are of interest as possible components in nanoscale electronic circuits. Both the structural and electronic properties can be augmented by packing tubes together into a bundle or *rope* of tubes. Recently, crystalline ropes of single-wall nanotubes have been synthesized with high yields. X-ray diffraction studies and transmission electron microscopy (TEM) pictures show that the ropes are formed of tubes whose diameter is narrowly dispersed around that of a (10,10) tube and that are packed into a triangular lattice with an intertube spacing similar to that between the atomic layers in graphite.[5] It then becomes necessary to inquire whether the interactions between the nanotubes substantially perturb the electronic properties of the rope and render it different from a simple summation of the properties of the individual nanotubes. In this paper, we will address this question using both empirical pseudopotential[6] and *ab initio* pseudopotential density-functional theory calculations.[7,8] The essentials of our work are described in Ref. 9, and in this paper we shall provide a fuller account of the method and results. We note that the work reported in Ref. 9 has since been confirmed.[10]

Much of the properties of nanotubes can be deduced from those of graphene, which is a single sheet of graphite, and so we shall initially discuss the band structure of graphene and graphite. The difference between graphene and graphite will provide us with an estimate for the likely strength of intertube coupling, and with this motivation we shall then describe our calculational schemes. The results of our calculations will then be described and explained, and finally, we shall summarize our findings and the effects they lead to for ropes of metallic nanotubes.

II. GRAPHENE, GRAPHITE, AND NANOTUBES

In Figs. 1 and 2, we show the Brillouin zone and band structure of a sheet of graphene. We are most interested in the behavior of the two bands that touch at the six corners of the hexagonal zone, and have linear dispersions in a range of several eV around the Fermi level, which is right at the intersection of these two bands. These bands are derived from the one p_z orbital per carbon atom which is not involved in

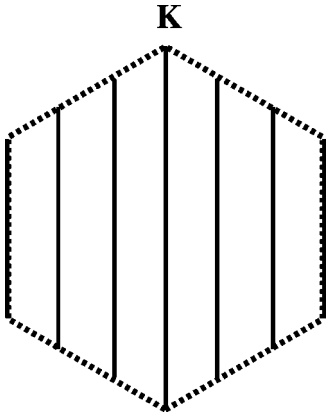

FIG. 1. Brillouin zone for graphene, with the allowed k vectors for a (3,3) nanotube plotted with the solid lines.

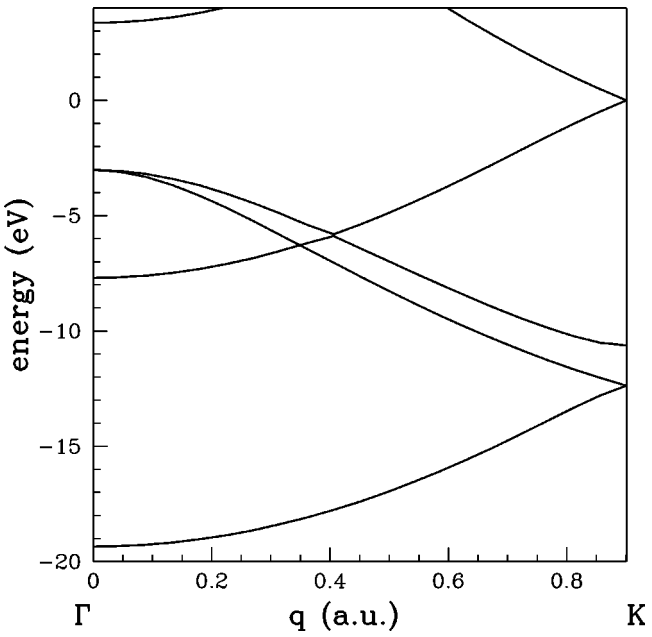

FIG. 2. Graphene band structure from Γ to *K*, with the Fermi level set to zero.

the sp^2 in-plane bonds, and can be considered as bonding (valence band) and antibonding (conduction band) combinations of these π orbitals. The one electron per atom not involved in the in-plane σ bonds fills up the valence band, producing zero-gap or semimetallic behavior. We note that around either of the two distinct corner points, the energy dispersion in any direction $\delta\mathbf{k}$ away from the corner is linear with the same slope, and so the energy bands there are conical to a good approximation.

There are many ways of cutting and rolling a sheet of graphene to form a tube, and the standard scheme for indexing the resulting tubes is by specifying the roll-up or circumference vector **c** in terms of its two integer coefficients with respect to the lattice vectors of the graphene sheet, $\mathbf{c}=n\mathbf{a}_1+m\mathbf{a}_2$. In this paper, we shall be studying the metallic armchair tubes that have one out of every three carbon-carbon bonds running along the circumference of the tube. These have roll-up indices (n,n), and in particular we shall be studying the (10,10) nanotube because its diameter is consistent with the x-ray and TEM measurements for tubes in the observed ropes.[5]

A good approximation to the band structure of a particular tube may be derived by selecting from the graphene band structure only those wave functions $\psi_{n\mathbf{k}}$ that already obey the required periodic boundary conditions across what will become the circumference of the tube.[2–4] This condition generates lines of allowed **k** values in the graphene Brillouin zone, which we illustrate in Fig. 1 for a (3,3) armchair tube. For any (n,n) nanotube, the point *K* at the corner of the zone where the conduction π^* and valence π bands touch is always allowed, and this means that an (n,n) nanotube should be metallic, as claimed above, with a one-dimensional band structure as shown schematically in Fig. 3. In one dimension, these two bands that cross in a linear fashion at the Fermi level will yield a constant density of states (DOS) in a region about 1.5-eV wide around the Fermi level, and a constant joint density of states (JDOS) from 0 to around 1.5 eV. From

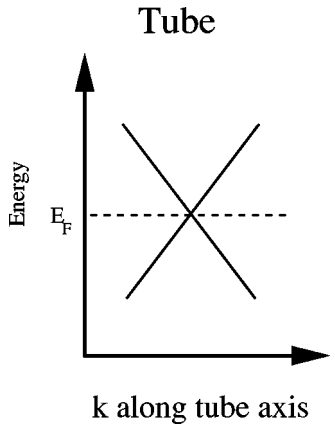

FIG. 3. Schematic band structure for a (n,n) carbon nanotube.

the point of view of symmetry, the crossing of these two bands is allowed because an isolated (n,n) nanotube has *n* mirror planes, which include the tube axis, and so the eigenstates can be chosen to be of definite parity under at least one of those planes. For an armchair nanotube the conduction and valence bands turn out to be of opposite parity under this mirror operation. If one uses $k\cdot p$ theory to evaluate any possible band repulsion, this symmetry means that the matrix element $\langle c|\delta k\cdot p|v\rangle$ which occurs in the second order of perturbation vanishes, and so the bands do not repel. The breaking of this symmetry in a rope could change the physics of the rope and qualitatively change the electronic structure near the Fermi level.

To get an estimate of the strength of the tube-tube interaction, it is natural to examine the effects of the interlayer interactions on the band structure of graphite. In Fig. 4, we display a calculated local-density approximation (LDA) band structure of graphite, which shows the large ($\simeq$1.5 eV) splitting at Γ between the two valence π bands and the splitting at *K* (due to interlayer effects) of 1.4 eV between the

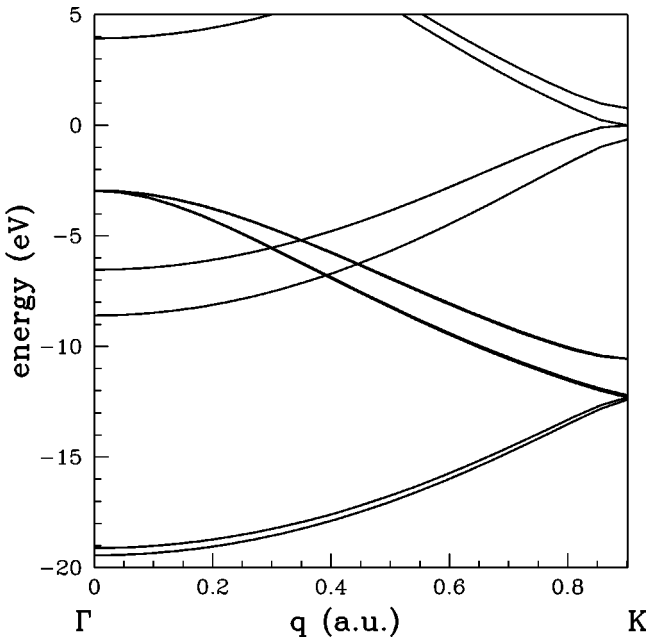

FIG. 4. Graphite band structure from Γ to *K*, with the Fermi level set to zero.

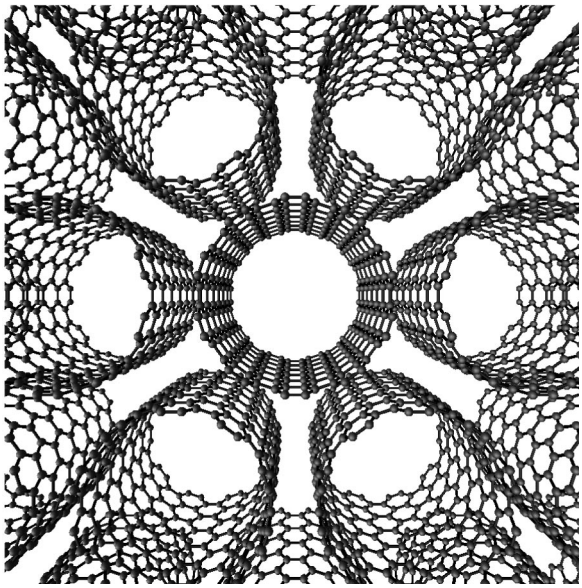

FIG. 5. A view down the axis of a rope of (10,10) nanotubes, with both axial mirror planes visible.

upper π^*-derived conduction band and the lower π-derived valence band. As K is the point in the Brillouin zone from which the states at the Fermi energy in the metallic tubes are derived, we could expect the tube-tube interaction to be of roughly this magnitude. In the ropes, due to the curvature of the tube walls, each tube is covered less effectively by the neighboring tubes and so this should weaken the intertube coupling compared to that in graphite. Still, the remaining tube-tube interactions in the rope could be expected to be strong enough to produce significant changes in the rope's electronic properties.

III. CALCULATIONS

We now turn to a description of the calculations we performed to get a more precise estimate of the strength of the tube-tube interactions and their effects on the band structure of the rope. The structure we studied consisted of an infinite lattice of (10,10) carbon nanotubes, arranged in a triangular lattice with their axes along the vertical or z direction.[5] The intertube distance was taken to be 3.3 Å. Initially, we studied the most highly symmetric situation where the tubes were rotated about their axes so that the structure as a whole still has some vertical mirror planes. This structure was generated by taking one tube per unit cell and then by rotating all of the tubes simultaneously until one of the vertical chains of hexagons running up the side of a tube lines up exactly with a similar chain in the side of the neighboring tube to the right. Axial symmetry through the axis of the center tube then implies that the diametrically opposite hexagon chain also lines up exactly with the neighboring tube on the left. With (10,10) tubes as the constitutive units in the rope, it is not possible to go further and arrange for a line up with the other four neighboring tubes. This situation is depicted in Fig. 5. As can be seen by inspection, there are two vertical mirror planes, one along the x axis, which goes through the centers of the aligned hexagon chains, and one perpendicular to this along the y axis. The point group of the structure is D_{2h}, which has eight elements and is generated by these two mirrors and the inversion. Then, to study the effects of orientational disorder, we rotated each tube by 1.5°, hence breaking all the vertical mirror symmetry by losing these two vertical mirror planes and producing a misaligned structure. The point group now is C_{2h}, whose four elements can be generated from the inversion and a rotation through 180° about the tube axis.

We used two computational schemes to study the rope band structure: *ab initio* pseudopotential density functional theory[7] in the local-density approximation (LDA) and the empirical pseudopotential method (EPM).[6] The latter was used for the bulk of our work because it is much faster than the LDA calculation: graphite naturally requires a large energy cutoff and nanotube calculations tend to have a large unit cell, so in the LDA calculation the matrices we need to diagonalize are very large. By using the EPM, we reduce the size of the matrices by a factor of 10, and this allows us to compute quantities such as the density of states, for which we need band-structure information on a mesh of k points in the irreducible part of the Brillouin zone. We used the more time-consuming LDA calculations to verify our EPM results at selected k points in the Brillouin zone.

We obtained our empirical pseudopotential by discovering a smooth curve in reciprocal space, which yielded a band structure for graphite and graphene, which agreed with theoretical and experimental results, with particular emphasis on the band structure near the Fermi level.[11] To quantify this agreement, we used an ''error'' function d, which was computed by taking sums of squares of differences between the target energy eigenvalues and our computed values, with weights selected so as to make d particularly sensitive to energies and energy gaps near the Fermi level. We selected a spherically-symmetric empirical pseudopotential $V(q)$ with seven parameters, and we determined the values of these parameters by varying them until we had minimized d, and so come to close agreement with our target eigenvalues. At the beginning of the fit, we encountered difficulties because the conduction bands kept on coming down in energy near Γ, but we were able to solve this problem by requiring that our potential reproduce the work function of graphite. This pulled the top of the valence bands 4.7 eV (Ref. 12) below the vacuum level, and separated them from the conduction bands at Γ. We ran our calculations with the resulting potential at a cutoff of 12.2 Ry.

To compute the DOS and JDOS for the aligned and misaligned structures that we studied, we needed to compute the band structure on a grid of k points in the irreducible Brillouin zones of the structures, which are, respectively, one eighth and one quarter of the full zone. For the aligned case, we used an adaptive grid of 22×23 k points, and for the misaligned structure 40×23 k points. We chose 22 and 40 k points, respectively, in the irreducible part of the $k_z=0$ hexagonal slice of the Brillouin zone of the rope, and then put 23 k points on each of the vertical lines, which ran up from these points, varying the spacing between these points so that the band-structure features that we observed along each line were sampled accurately. The tetrahedron method[13,14] was then used to compute both the DOS and the JDOS, after the Fermi level had been determined.

We confirmed our EPM band-structure results by doing a

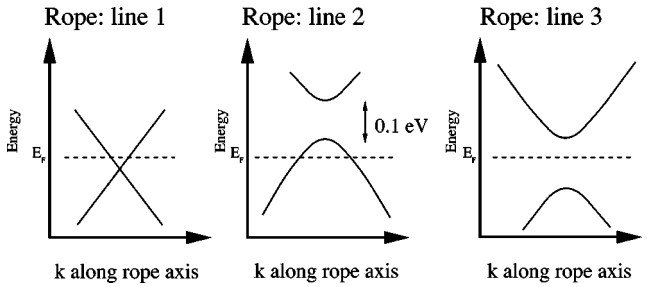

FIG. 6. A schematic display of the band structure of the rope along various lines in reciprocal space parallel to the tubes. The Fermi energy is shown by the dashed line.

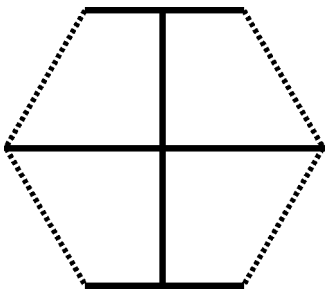

FIG. 7. The $k_z=0$ slice of the Brillouin zone of the rope, with each point on the bold lines indicating those vertical lines in reciprocal space where band crossing is permitted.

self-consistent *ab initio* pseudopotential density-functional theory LDA calculation on the rope, and then by examining the behavior of the conduction and valence bands along selected vertical lines in reciprocal space. In all cases, we found that the *ab initio* results were in good agreement with the EPM results. The *ab initio* calculations give almost identical **k** positions for the band crossings (or band minima and maxima) and within 20% of the magnitude of the band splitting in comparison to the EPM calculations.

IV. RESULTS

To discuss our results for the three-dimensional band structure of the rope of tubes, we shall plot the conduction and valence bands along some of the vertical lines in the Brillouin zone. In the limit in which the tubes in the rope are separated far away from each other, the band structure should be identical along any one of these lines, and equal to that of an isolated armchair tube, with two bands crossing linearly at the Fermi level as was shown in Fig. 3. At the actual tube-tube separation of 3.3 Å we expect to see some band dispersion in the horizontal plane.

A schematic presentation of our results is given in Fig. 6, where we plot the typical band structures we obtain for the aligned case along three representative lines in the Brillouin zone. Along the first line that passes through the center of the zone at Γ, we see the persistence of the band crossing that one observes in the isolated tube. Along the other two lines, which represent the general case, we find energy gaps opening up between the conduction and valence bands due to band repulsion, as could be expected from symmetry. This proves that indeed the tube-tube interactions break the important mirror symmetries of the isolated tubes, and establishes that the resulting perturbation changes the nature of the electronic physics at the Fermi level. In the figure, we illustrate the position of the Fermi energy by the dashed line. We see that along the vertical line through Γ we expect to find a pocket of electronlike states, while along the next line we expect to find a pocket of holelike states. We observe that the location and size of the gap vary from line to line, as we illustrate in the figure, so that along some vertical lines in the Brillouin zone of the rope (such as line 3 in the figure) neither holelike nor electronlike states are to be found. From this observation we can expect to find semimetallic behavior in a rope of (10,10) tubes, with both hole and electron pockets in the Fermi surface. We can also expect that the sparseness of electronic states near the Fermi level will reduce the density of electrons available for transport.

The allowed crossings occur along vertical lines in the Brillouin zone whose k vector is preserved under the two mirror symmetries that the aligned structure possesses. These crossings occur along any line whose intersection with the $k_z=0$ slice of the Brillouin zone for the structure of the rope of tubes (which is also hexagonal) lies on the indicated regions in Fig. 7, as these are clearly preserved by the two mirror symmetries modulo a reciprocal lattice vector. On lines which intersect the $k_z=0$ slice of the Brillouin zone near these points there is always a band gap, but it may be small.

For the misaligned case, we find energy gaps along every line in the zone, generally of size 0.1 to 0.3 eV. For both aligned and misaligned structures we graph the density of states in Fig. 8, calculated using the tetrahedron method. As can be confirmed from Fig. 6, in a region of around 0.1 eV at the Fermi level, we find a diminishment in the number of electronic states due to the band repulsion, and hence a valley or pseudogap in the DOS where the density of states falls to roughly 30% of the isolated tube value. This constant isolated tube level can be seen to the left and right of the

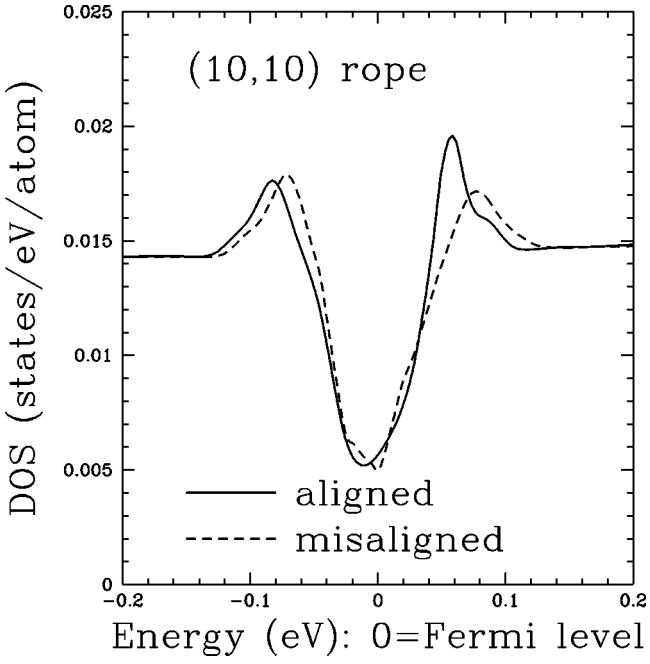

FIG. 8. The density of states of the rope of tubes, for both aligned and misaligned structures.

pseudogap in the figure. The DOS does not completely disappear because the energy dispersion in the horizontal plane moves the location and energy of the gap around, and so due to the resulting band overlap there will always be some states in the energy region of interest. A sufficiently high pressure applied to a section of the ropes could increase the energy gaps sufficiently to separate conduction and valence bands fully, leading to a semiconducting rope. Such a pressure dependence of the conductivity might make the rope useful as a pressure gauge. Also, any general strong external perturbation would cause a larger band repulsion, which could explain the quantum dot behavior of isolated tubes and ropes,[15,16] where a semiconducting barrier region seemingly develops at the contact where just such a strong perturbation is expected.

As the figure shows, the density of states for the aligned and misaligned structures show very similar behavior. This is because the regions where the aligned band structure differs from the misaligned cases cover only a small percentage of the zone volume, and so we see no significant change between the two curves. This leads to the important conclusion that the DOS (and hence properties related to it) does not depend significantly on the details of the relative orientation of the tubes. On the other hand, these ropes should be sensitive to doping concentrations that would determine the position of the Fermi level inside the pseudogap, and also to temperature, which would lead to the electrons sampling the DOS at energies where the DOS is rapidly varying.

As was proved in the discussion surrounding Fig. 6, the actual Fermi surface produced by the π-bonding and π-antibonding states is composed of both electronlike and holelike pockets. Under the assumption of the highest possible symmetry (aligned case) we find a flat (in the rope axis direction) pocket of electronlike states in the shape of a rhombic pancake, and a pocket of holelike states in a similar shape. The pocket of electronlike states intersects the vertical line through Γ, as can be deduced from Fig. 6, while the pocket of holelike states is situated more towards the edge of the zone. Actual ropes have disturbances in their periodic structure and in the relative orientations of the constituent tubes, and so we expect that in such ropes these Fermi surfaces would be smeared out to some degree. The temperature dependence of the thermopower and Hall effect should be rather complicated because of the presence of both electron and hole carriers as well as this partial smearing out of the Fermi surfaces.

The joint density of states for the aligned and misaligned structures is plotted in Fig. 9, where we see the appearance of a true gap starting at zero energy. To understand the physics of this, we consider the defining equation of the JDOS,

$$\mathrm{JDOS}(E)=\sum_{o,u}\frac{1}{4\pi^3}\int_{\mathrm{B.Z.}} d^3k\,\delta(E_k^u-E_k^o-E), \qquad (1)$$

where o and u run over the occupied and unoccupied states respectively. For a single tube where the three-dimensional integral is replaced by a one-dimensional integral, the two linear bands at the Fermi level will generate a constant JDOS, at least up to energies of the order of an eV away from zero. Because **k** conservation is exact for our three-dimensional infinitely wide and long rope, a photon can only cause vertical **k**-conserving transitions, as the above equation expresses, and so except for the measure zero set of high-symmetry points, the band repulsion makes sure that there is always an energy gap present between any initial state and an allowed final state. This is what causes the gap that shows up in the JDOS for both structures, which should be detectable using infrared absorption measurements. However, we also note that the assumption of vertical **k**-conserving transitions used above may have to be relaxed in the study of ropes. As a real rope does not have a perfectly periodic structure, **k** conservation is only approximately valid, and so there may be some weight in the gap region due to transitions between states that are not allowed for a perfect rope. In the extreme case of complete disorder, an infrared experiment would reflect a plot similar to the DOS rather than the JDOS. So, for a finite rope of metallic nanotubes, we expect features in-between the JDOS prediction of a true gap of width a few tens of meV and the DOS prediction of a pseudogap.

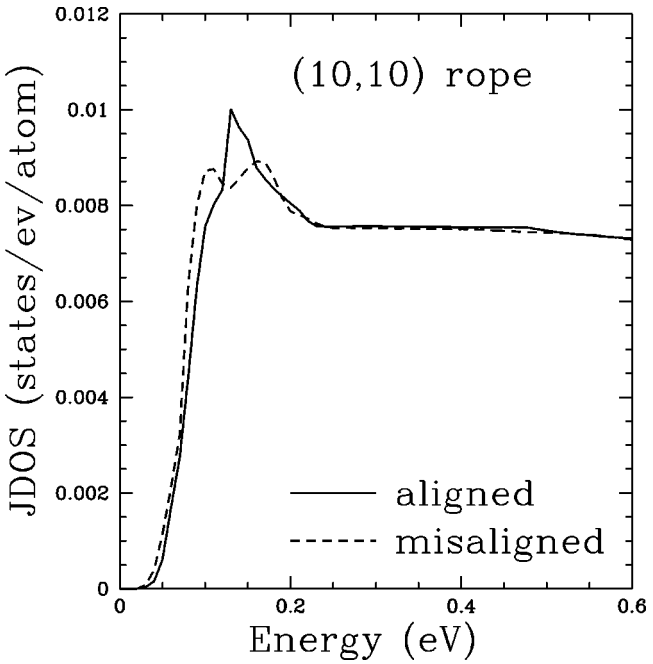

FIG. 9. The joint density of states of the rope, for both structures.

V. CONCLUSION

We now summarize our findings and suggest some avenues for future research. We have shown that tube-tube interactions in ropes of armchair carbon nanotubes strongly influence the electronic band structure of the tubes near the Fermi level, and cause quantum-mechanical band repulsion, splitting the conduction and valence bands by a gap of order 0.1 eV. Due to the dispersion in the plane perpendicular to the axis of the rope, semiconducting behavior is avoided and instead, we predict that the rope should become a semimetal, with both electron and hole carriers and a diminished density of states at the Fermi level. The carrier mobility at the Fermi level should also be reduced. These features should make the rope very sensitive to doping and should cause a strong temperature dependence in the conductivity and other properties. More of a semimetallic character should be observed, espe-

cially in Hall effect and thermopower measurements, due to the existence of both hole and electron carriers. The joint density of states reveals that the band repulsion should have as signature a diminishment of weight in the infrared absorption spectrum, with a perfect rope having a true gap in the JDOS starting at zero and extending up to a few tens of meV.

Although our study was for a rope of metallic tubes, we predict similar band repulsion for any armchair tube interacting strongly with a surface or with other nonarmchair tubes, such as in a mixed rope. It would be interesting to see the experimental dependence of this effect on the proximity of the perturbing body, and we suggest that the pressure dependence of conducting ropes would be interesting to study, with an eye to using them as a pressure gauge.

ACKNOWLEDGMENTS

We thank V. Crespi for providing us with relaxed atomic coordinates. This work was supported by the National Science Foundation Grant No. DMR-9520554 and by the Director, Office of Energy Research, Office of Basic Energy Sciences, Materials Sciences Division of the U.S. Department of Energy under Contract No. DE-AC03-76SF-00098.

*Also at the Department of Physics and Center for Theoretical Physics, Seoul National University, Seoul 151-742, Korea.

[1] S. Iijima, Nature (London) **354**, 56 (1991).
[2] N. Hamada, S. Sawada, and A. Oshiyama, Phys. Rev. Lett. **68**, 1579 (1992).
[3] J.W. Mintmire, B.I. Dunlap, and C.T. White, Phys. Rev. Lett. **68**, 631 (1992).
[4] R. Saito, M. Fujita, G. Dresselhaus, and M.S. Dresselhaus, Appl. Phys. Lett. **60**, 2204 (1992).
[5] A. Thess, R. Lee, P. Nikolaev, H. Dai, P. Petit, J. Robert, C. Xu, Y.H. Lee, S.G. Kim, A.G. Rinzler, D.T. Colbert, G.E. Scuseria, D. Tomanek, J.E. Fischer, and R.E. Smalley, Science **273**, 483 (1996).
[6] M.L. Cohen and J.R. Chelikowsky, *Electronic Structure and Optical Properties of Semiconductors* (Springer-Verlag, Berlin, 1988), p. 20.
[7] P. Hohenberg and W. Kohn, Phys. Rev. **136**, B864 (1964).
[8] S. Fahy, S.G. Louie, and M. Cohen, Phys. Rev. B **34**, 1191 (1986).
[9] P. Delaney, H.J. Choi, J. Ihm, S.G. Louie, and M.L. Cohen, Nature (London) **391**, 466 (1998).
[10] Y.-K. Kwon, S. Saito, and D. Tomanek, Phys. Rev. B **58**, R13 314 (1998).
[11] J.-C. Charlier, J.-P. Michenaud, and X. Gonze, Phys. Rev. B **46**, 4531 (1992).
[12] R.F. Willis, B. Fitton, and G.S. Painter, Phys. Rev. B **9**, 1926 (1974).
[13] G. Lehmann and M. Taut, Phys. Status Solidi B **54**, 469 (1972).
[14] G. Gilat and N.R. Bharatiya, Phys. Rev. B **12**, 3479 (1975).
[15] S.J. Tans, M.H. Devoret, H. Dai, A. Thess, R.E. Smalley, L.J. Geerligs, and C. Dekker, Nature (London) **386**, 474 (1997).
[16] M. Bockrath, D.H. Cobden, P.L. McEuen, N.G. Chopra, A. Zettl, A. Thess, and R.E. Smalley, Science **275**, 1922 (1997).